Advanced Steel Construction – Vol. 18 No. 2 (2022) 617–629
DOI:10.18057/IJASC.2022.18.2.10

EFFECTS OF THE NUMBERS OF STORIES AND SPANS ON THE COLLAPSE-RESISTANCE PERFORMANCE OF MULTI-STORY STEEL FRAME STRUCTURES WITH REDUCED BEAM SECTION CONNECTIONS

Zheng Tan [1], Wei-Hui Zhong [1, 2], Li-Min Tian [1, *], Yu-Hui Zheng [1], Bao Meng [1], Shi-Chao Duan [1] and Cheng Jiang [1]

[1] *School of Civil Engineering, Xi'an University of Architecture and Technology, Xi'an 710055, China*
[2] *Key Laboratory of Structural Engineering and Earthquake Resistance, Ministry of Education, Xi'an University of Architecture and Technology, Xi'an 710055, China*
(Corresponding author. E-mail: tianlimin@xauat.edu.cn)

ABSTRACT

The progressive collapse of a building structure under an accidental load involves a relatively complex mechanical behavior. To date, the collapse of single-story beam-column assemblies has been investigated extensively, revealing the resistance development of beams during progressive collapse. However, few studies of the progressive collapse behavior of multi-story frame structures have performed a systematic analysis of the Vierendeel action (VA) at a comprehensive level. It is difficult to convert quantitative analysis results accurately from the component level to the overall structure level to evaluate the collapse resistances of structures. To investigate the effects of the numbers of stories and spans on the collapse resistances of steel frame structures, a refined numerical simulation study of a multi-story frame model with different numbers of stories and spans was performed. First, the correctness of the finite element modeling method was verified by the collapse test results of a single-story and two-story frame. Then, the finite element modeling method was applied to study the collapse resistances of multi-story frame structures with different stories and spans. The load–displacement response, internal force development, deformation characteristics, and resistance mechanisms were analyzed, and the contributions of the flexural and catenary mechanisms of each story were separated quantitatively. The results illustrated that the VA can improve the load-carrying capacity to a certain extent in the small deformation stage, but can also cause the frame structures to undergo progressive collapse from the failure story to the top story. The bearing capacity of the multi-story frame did not have a simple multiple relationship with the number of stories. Increasing the number of spans can improve the collapse resistance in the large deformation stage, which is more obvious when the number of stories is smaller, and this accelerates the upward transmission of the axial tension force among the stories, although this effect is minimal for frames with few stories.

ARTICLE HISTORY

Received: 2 June 2021
Revised: 6 December 2021
Accepted: 21 December 2021

KEYWORDS

Progressive collapse;
Numerical simulation;
Number of stories;
Number of spans;
Vierendeel action

1. Introduction

Progressive collapse refers to the damage of a initial local failure of a structure by an accidental event (such as an explosion, earthquake, impact, fire, etc.), creating a chain reaction that spreads to peripheral frame, causing damage that is disproportionate to the initial damage range of the structure, and even leading to overall collapse of buildings [1-3]. Related research on progressive collapse started after the gas explosion of Ronan Point apartment. Subsequently, the overall collapse of the Alfred P. Murrah Federal Government Building due to a car bomb attack and the plane impact terrorist attack on the World Trade Center accelerated research on structural progressive collapse. With the trend of large and complicated building structures and increasing accidental disasters, building structure collapses are becoming increasingly frequent and have attracted widespread attention. Means of ensuring the overall stability of structures under the action of accidental loads has become a research focus of structural engineering [4].

In the past 10 years, scholars have conducted extensive studies on the progressive collapse resistances of frame structures. The existing research is mainly focused on the key parameters such as the connection types [5–9], boundary conditions [10, 11], composite action [12, 13], reinforcement ratios [14], and span-to-depth ratios [15–17]. These valuable investigations initially revealed the resistance mechanisms of beam members based on the alternate load path (ALP) method [1], but the previous collapse experimental studies had the following problems. (1) Considering economy and laboratory conditions, collapse performance has been investigated in scale tests, but the scale has a significant effect on the collapse behavior of the structure. (2) Single-story beam-column assemblies have generally been employed for progressive collapse analysis, and relevant studies preliminarily revealed the development law of the resistance mechanism of beam members. However, few studies have involved systematic analysis of multi-story frame structures on an overall level, making it difficult to convert the quantitative analysis results accurately from the component level to the structure level to elucidate the total resistance. (3) The horizontal boundary restraints of the side columns of beam-column assemblies are usually simplified [5, 7, 18] even without considering the boundary effect [19]. In general, the overhanging beams are connected with the gantry mounting, reaction frame, or reaction wall (see Fig. 1) through the rigid members to simulate the tie effect from the indirect influence area to the beam–column assembly. However, due to the uncertainty of the lateral stiffness of the horizontal tie device, the actual boundary conditions may be quite different.

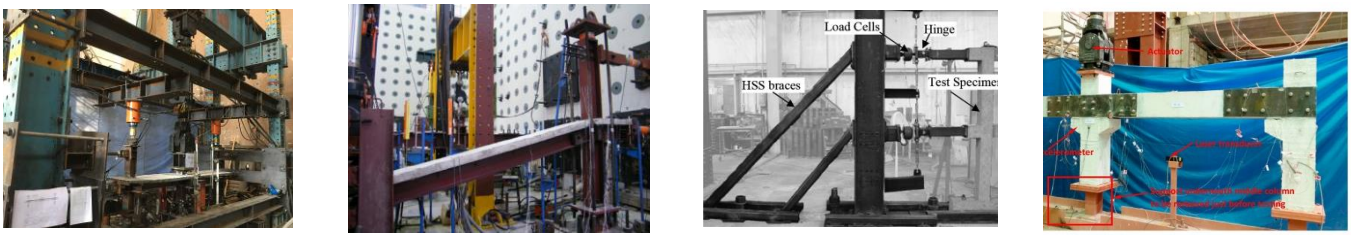

(a) Gantry mounting [5] (b) Reaction wall [7] (c) Reaction frame [18] (d) Without restraint [19]

Fig. 1 Typical simplification of boundary constraints in previous collapse tests

Previous studies have demonstrated that owing to the presence of the Vierendeel action (VA) [20, 21], the internal force redistribution and the mechanism development of each story are not identical. Thus, it is very unreasonable to replace the collapse-resistant performance of an actual multi-story frame structure directly with the analysis results of single-story beam-column assemblies. However, the VA has often been ignored when evaluating the collapse behavior, which is inconsistent with the actual situation. Regarding the multi-story plane concrete frame structure, Yi et al. [22] tested a

four-span, three-story reinforced concrete plane frame, and proposed a brief plastic analysis method for the collapse failure of frames. They concluded that the bearing capacity in the catenary mechanism stage was about 40% higher than that of the plastic stage. It was considered safe to predict the collapse resistance of a reinforced concrete frame by using the failure load of the plastic mechanism. Baghi et al. [23] performed related collapse experimental tests in the case of center column failure in order to investigate the role of infilled walls on the structural resistances of multi-story concrete frame structures. The study indicated that the existence of infilled walls could significantly improve the bearing capacity of the structure and change the original failure mode. Regarding multi-story flat steel frame structures, Wang et al. [24] and Qian et al. [25] reported collapse tests on two-story, two-bay steel frames with different types of connections, indicating that the connection types have important effects on the structural collapse resistance. However, they did not analyze the effects of VA on the collapse resistance. Tsitos et al. [26] studied two 1/3-scale, two-bay, three-story steel frames, incorporating a special moment resisting frame and a post-tensioned energy dissipation frame, respectively. However, as the tests did not consider the boundary constraint provided by the surrounding frames for the sub-frames, the side columns inclined inward severely in the catenary stage, which is considerably different from the structural response of an actual multi-story frame structure after the failure of the middle column. Chen et al. [27] studied the collapse behavior of a two-bay, two-story composite frame upon sudden column withdrawal. However, the strain of the structural members was far less than the yield strain, and the structural response in the large deformation stage could not be obtained. Sasani et al. [28] removed the inner bottom column of a 20-story reinforced concrete structure and evaluated and analyzed its anti-collapse capacity, finding that the VA plays a critical role in the anti-collapse of multi-story structures. Most of the above multi-story space frame tests have only included the stages through the elastic stage, and the structural behavior in the large deformation stage has not been obtained.

Although a considerable amount of valuable research has been reported and the collapse resistances of frame structures have increased substantially in recent years [29, 30], most research is still focused on beam-column assemblies. Hence, there remains a lack of research on the behavior of multi-story frame structures. Moreover, the overall internal force transfer and the development law of the load-resisting mechanisms between the beams and columns must be studied further; in particular, the effects of important parameters such as the numbers of stories and spans on the collapse behavior of multi-story frame structures require additional investigation. As it is difficult to perform collapse tests on frame structures with the number of stories and spans as related parameters owing to limited laboratory conditions and high cost, it is necessary to employ the finite element analysis method to evaluate the effects of the numbers of stories and spans on the collapse resistances of frame structures quantitatively. Therefore, the numerical modeling methods based on shell elements were verified in this study by comparing the test results obtained for the single-story beam-column assembly of Dinu et al. [6] and two-story sub-frame of Qian et al. [25]. In addition, parametric studies were conducted to investigate the collapse resistance, including the load–displacement response, internal force development, deformation characteristics, and resistance mechanisms of frame structures with different numbers of stories and spans. The conclusions drawn from the numerical simulation shed light on the evolution laws of internal forces between individual stories of frames against progressive collapse for different numbers of stories and spans, which could provide valuable reference information for engineers designing multi-story frames to resist progressive collapse.

2. Establishment and verification of finite element model (FEM)

2.1. Design of multi-story steel frame

According to the steel structure design standard GB 50017-2017 [31], an n×4-span multi-story steel frame, a 3×m span frame, and a 9×m span frame were designed, and the effects of the numbers of stories (n) and spans (m) on the collapse resistances of the multi-story frames were studied. Fig. 2(a) shows the model dimensions. The designed dead load (DL) and live load (LL) of the structure are 5.0 and 2.5 kN/m^2, respectively. The beam span and story height of the frame structures were 6000 mm and 3000 mm, respectively. Through structural design analysis, the beam and column sections were selected to be H400 × 200 × 8 × 13 (mm) and H450 × 300 × 11 × 18 (mm), respectively. The connection employed in the models was the reduced beam section welded connection (RBS), and Fig. 2(b) depicts the details of the connection. The connection has good ductility, which is conducive to structural displacement development in the catenary stage and widely employed in actual steel structure buildings. The beam end flange is weakened according to ANSI/AISC 358 [32], and Fig. 2(b) shows the specific weakening parameters of the flange. The values of the parameters a, b, and c were 120, 300 and 40 mm, respectively, where a represents the distance between the start of the RBS cut and the column flange, b is the length of the RBS cut, and c is the depth of the RBS cut.

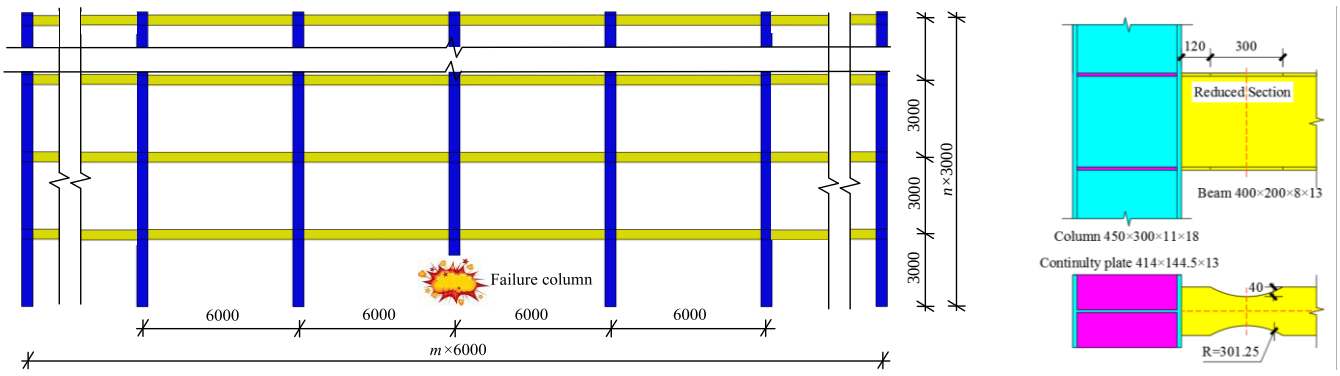

(a) Model dimensions (b) Connection details

Fig. 2 Simplified diagram of typical boundary constraints in previous collapse tests

2.2. Finite element modeling method

The ABAQUS/Explicit numerical simulation was employed to analyze the collapse resistances of the multi-story plane frame structures. This method can solve the nonlinear simulation problem effectively. To make the calculation results meet the static analysis requirements, the kinetic energy of the models should be controlled to be within 5–10% of the internal energy [33]. The modeling details are as follows.

2.2.1. Boundary conditions and meshing

To save calculation resources, all beams and columns adopted S4R shell elements. The beams and columns were connected by the "tie" command. As the specimen size and boundary constraint conditions were completely symmetrical, the 1/2 model was employed for modeling. Fig. 3(a) shows the numerical FEM and boundary constraint (taking the 3×4 model as an example). The restraints were employed to limit the out-of-plane deformation of the failed column and side columns and to ensure vertical movement.

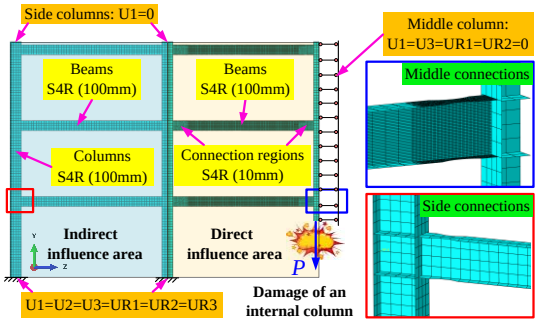

Fig. 3 Detailed information of the modeling process

The displacement control was adopted at the top of the failed column

[24-26] in the loading process until the model lost its load, and the amplitude attribute was the smoothing analysis step. The boundary condition at the bottom of the side columns was fixed constraint. The key area of the connection was divided into dense grid elements, which was about 10 mm. A 100 mm grid was adopted for the remaining beams and columns.

2.2.2. Constitutive models and fracture parameters

The steel was Q235, the yield strength was 235 MPa, the tensile strength was 353 MPa (the strength yield ratio was 1.5), and the elastic modulus E and Poisson's ratio were 206 GPa and 0.3, respectively. The stress–strain relationship of steel was defined by the four-stage constitutive model of secondary flow-plasticity [15].

To simulate the fracturing of steel during the collapse process, the ductile metal failure criterion and element deletion method in ABAQUS were used. The fracture strain, triaxial stress, strain rate, and other parameters of the steel material were defined to simulate the steel fracture. The element deletion method was used in the simulation. When the equivalent elastic strain exceeds the fracture strain, the element was deleted automatically. The relationship between equivalent plastic damage strain and stress triaxiality was as follows [34]:

$$\bar{\varepsilon}_0^{pl} = \begin{cases} \infty, & \eta \le -1/3 \\ C_1/(1+3\eta) & -1/3 \le \eta \le 0 \\ C_1 + 9(C_2 - C_1)\eta^2 & 0 \le \eta \le \eta_0 \\ C_2/3\eta & \eta_0 \le \eta \end{cases} \quad (1)$$

Here, $\bar{\varepsilon}_0^{pl}$ is the equivalent plastic damage strain of steel, η is the stress triaxiality, and C_1 and C_2 are $\bar{\varepsilon}_0^{pl}$ under pure shear and under uniaxial tension, respectively, and can be calculated by Eqs. (2)~(4):

$$C_2 = -\ln(1 - A_R) \quad (2)$$

$$C_1 = C_2(\sqrt{3}/2)^{1/n} \quad (3)$$

$$\sigma = K(\varepsilon)^n, \quad (4)$$

where A_R is the reduction in area and K and n are the hardening parameters of steel.

2.3. Verification of FEM

The collapse tests of a single-story beam-column assembly [6] and a two-story sub-frame [25] were selected as the basis for the verification of the numerical simulation modeling method in this study.

2.3.1. Single-story frame

Dinu et al. [6] performed a quasi-static collapse test on a two-span three-column single-story beam-column assembly with RBS connection. The specimen scale was 3/8, and the span was 3000 mm. Table 1 lists the material properties of steel members. The beam and column dimensions were H220 × 220 × 5.9 × 9.2 (mm) and H260 × 260 × 10 × 17.5 (mm). The connection used in the models was RBS, and Fig. 4 illustrates the test loading setup and beam-to-column connection. Considering the effects of the surrounding frame on the direct influence area, two sides of the specimen were connected to the reaction wall and reaction frame, respectively. A vertical load was applied to the top of the failed column through a 100T hydraulic servo actuator, and several vertical columns were installed along the beam span to prevent out-of-plane displacement.

Table 1
Properties of the steel members [6].

Members	f_y (MPa)	f_u (MPa)	f_f (MPa)	A_{gt} (%)
Beam flange	351	498	357	15.0
Beam web	370	497	400	15.0
Column flange	402	583	481	12.9
Column web	393	589	532	13.3

Note: f_y is the yield strength, f_u is the ultimate strength, f_f is the fracture strength, and A_{gt} is elongation.

Fig. 4 Collapse test of one-story steel frame with RBS connection [6] (dimension units: mm)

According to the specific dimensions of the specimen in reference [6], the corresponding model was established, as shown in Fig. 5. It should be noted that to consider the horizontal constraints of the restraint device for the side connections of the specimen, the numerical model needed to set the boundary springs in the two side connections, the corresponding axial stiffnesses were 308 kN/mm and 95 kN/mm, and the gaps between the pin and hinged joint was 2.8 mm and 7 mm, respectively.

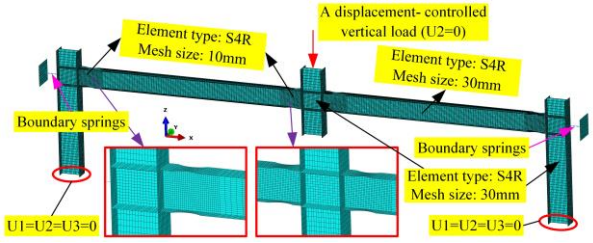

Fig. 5 FEM of the single-story beam-column assembly

Fig. 6(a) compares the FEM and test results. It can be observed that the load–displacement curves obtained from the FEM closely coincide with the test curves. The final fracture displacement and load in the numerical simulation are 472 mm and 431 kN, respectively, and the corresponding test results are 480 mm and 401 kN, respectively. The errors are less than 7%, indicating that the FEM is reliable. Fig. 6(b) illustrates the failure mode of the specimen obtained from the finite element simulation. Both the numerical simulation and experimental test reveal fractures at the weakened flange of the side joint, which demonstrated that the FEM can accurately simulate the failure process of the RBS connection of the single-story beam-column assembly subjected to a middle column loss.

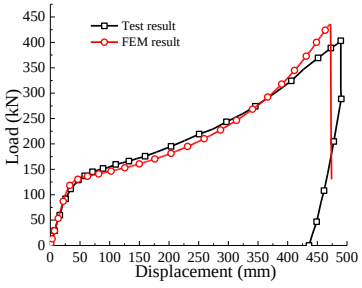

(a) The load-displacement curve

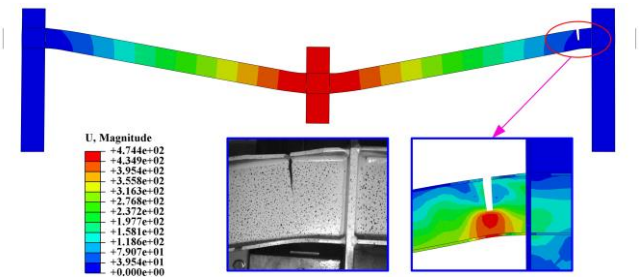

(b) Failure mode

Fig. 6 Comparison of the results of the single-story beam-column assembly from FEM and test

2.3.2. Two-story frame

Qian et al. [25] tested a 1/2-scale, two-bay, three-column, two-story sub-frame with RBS connections. Fig. 7 shows the loading device and details of the RBS connections. The beam span of the specimen is 3000 mm, the length of the extended beam is 655 mm, the story height is 1500 mm, the beam and column sizes are H150 × 150 × 7 × 10 (mm) and H200 × 100 × 5.5 × 8 (mm), respectively. The details of the specimen sizes are provided in reference [25]. The steel is Q235, and Table 2 lists the specific properties of each part of the specimen. The bottoms of the two side columns are connected with hinged connectors fixed to the ground by bolts, and the outrigger of each story is connected with the A-frame to simulate peripheral constraints. At the top of the failed column, the vertical load applied by the jack is used to simulate the loss of an internal column until the specimen is completely destroyed. The specimen was restrained by the lateral steel column to prevent lateral instability, and two-point loads (the axial compression ratio was selected to be 0.3) were applied to the tops of the side columns to consider the upper load from the stories above.

Table 2
Properties of the steel members [25].

Members	f_y (MPa)	f_u (MPa)	f_f (MPa)	A_{gt} (%)
Beam flange	310	420	315	12.0
Beam web	320	430	340	13.5
Column flange	300	410	300	14.0
Column web	295	375	265	13.0

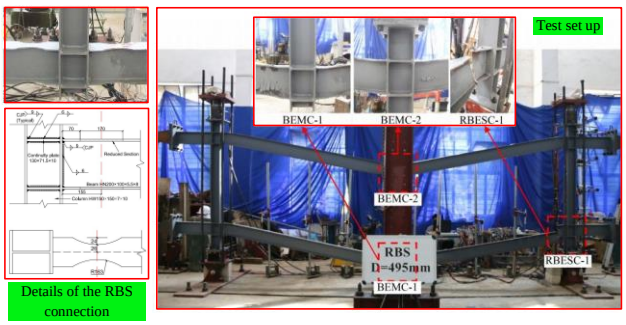

Fig. 7 Collapse test of two-story steel frame with RBS connection [25] (dimension units: mm)

The FEM was established according to the detailed size of the specimen in the literature, as shown in Fig. 8. To simulate the influence of the surrounding members on the collapse resistance of the beam-column assembly, the boundary springs were used to simulate the horizontal constraints at the overhanging beams. The axial stiffnesses of the side joints at the first and second story were 39.2 and 31.0 kN/mm, and the gaps were 0.7 and 0.9 mm, respectively.

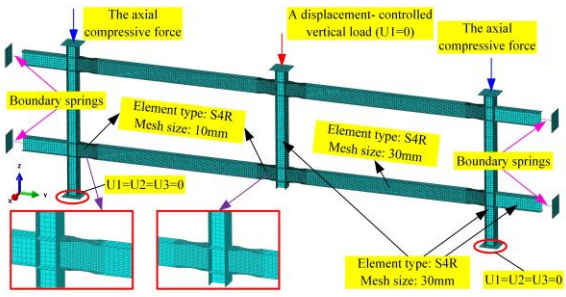

Fig. 8 FEM of the two-story sub-frame

The comparison between the FEM and the test results of the two-story frame is illustrated in Fig. 9. As shown in Fig. 9(a), the load–displacement curve obtained by the numerical model is close to the test curve. The initial stiffness and plastic load are almost the same, and the error between the peak load and corresponding displacement (437 mm, 364 kN) obtained by numerical simulation and the experimental value (463 mm, 330 kN) is less than 10%, which shows that the simulation results of dynamic quasi-static analysis method have enough accuracy, and they can better reflect the main stress characteristics of two-story frame under large deformation stage. The failure mode of the model is roughly consistent with the test, as illustrated in Fig. 9(b). Further, it shows that the dynamic quasi-static analysis method could well simulate the fracture behavior of multi-story frame specimens. Through the finite element analysis of the collapse test of single-story beam-column assembly and two-story sub-frame, the results demonstrated that the numerical simulation can accurately obtain the main load response and failure modes; thus, the modeling method can be used to explore the influence of the numbers of stories and spans on the collapse behavior of multi-story frame.

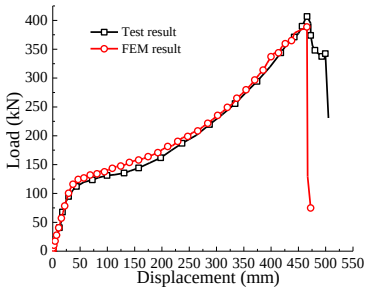

(a) The load-displacement curve

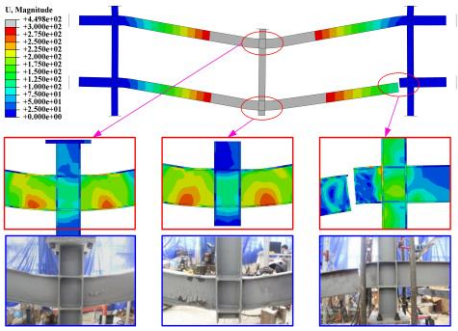

(b) Failure mode

Fig. 9 Comparison of the results of the two-story sub-frame from the test and FEM

3. Collapse resistances of frames with different numbers of stories

To study the effects of the number of stories on the collapse resistances of the structures, plane steel frames with RBS connections and from one to nine stories were taken as the research objects.

3.1. Load–displacement response

Fig. 10(a) illustrates the load–displacement curves of the frame structures with different numbers of stories with middle column removal. Clearly, as the number of stories increases, the initial stiffness and plastic load of the structure increase successively. Only the load development of the one- and two-story frames show constant increasing trends; that is, the collapse resistance in the large deformation stage exceeds the resistance provided by the small deformation stage. The other models reach the maximum load in the small deformation stage, and the load subsequently decreases as the displacement increases. Therefore, directly replacing the total resistance of a multi-story frame with that of a single-story frame structure will cause the resistance of the structure to be overestimated in the catenary mechanism stage, which is unsafe for the structural design. The dynamic response of the structure under sudden loading can be approximately obtained through the principle of energy balance [35] according to the structural load response under static loading. Fig. 10(b) depicts the pseudo-static curves of each model. The maximum pseudo-static load points can be adopted to determine whether the structure collapses. The maximum pseudo-static load points of the first and the second story frame appear in the large deformation stage, whereas the maximum pseudo-static load points of the others occur in the middle stage of loading. As shown in Fig. 10(c), the load–displacement curves of the 1×4, 3×4, and 9×4 models were compared using multiple relations. Compared with the 1×4*3 and 1×4*9 curves, the maximum loads in the small stage of the 3×4 and 9×4 models are increased by 11.9% and 4.1%, respectively. Further, compared with the 1×4*3 and 1×4*9 curves, the fracture loads of the 3×4 and 9×4 models in the large deformation stage are decreased by –48.3% and –68.8%, respectively. Compared with the 3×4*3 curve, the maximum load of the 9×4 model is increased by 4.1% and the fracture load is decreased by 40.0%. Thus, the VA can increase the collapse resistance to a certain extent in the small deformation stage, but not significantly.

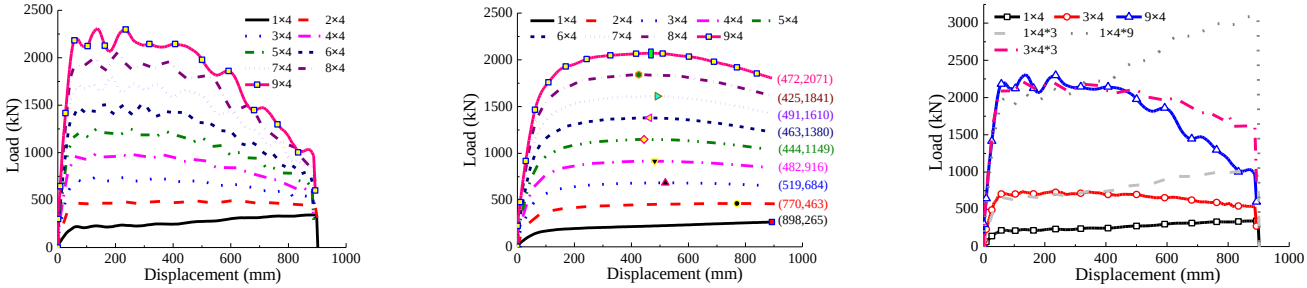

(a) The load–displacement curves (b) Pseudo-static curve-displacement curve (c) Multiple comparison (1×4, 3×4, 9×4)

Fig. 10 Structural load response of the frames with different stories

3.2. Evolution law of the internal force among the stories

Fig. 11 shows the axial force development of frame structures with different numbers of stories throughout the loading process. The axial force of the 1 × 4 model first presents a negative value, and the axial force becomes positive and develops rapidly until the tension flange at the beam end breaks as the displacement increases. For the multi-story frame structure, the distribution characteristics of the axial force of the beams in each story are not the same, which is quite different from the single-story frame structure case. The axial tension force of the multi-story frame is mainly concentrated in the failure story and can reach $0.35N_p$ ($N_p=f_yA$, where A is the area of the most unfavorable section of the beam). This force has the next-largest value in the second story ($0.1N_p$), and the top beams exhibit significant compressive forces, whereas the axial forces of the other stories are not obvious. According to the distribution characteristics of each story axial force, the failure beam and top beam are equivalent to the tension and compression areas of the Vierendeel beam, respectively; the middle stories can be regarded as the neutral layer; and the different directions of axial forces cause additional bending moments to resist the external load. It can be seen from the development trend of each story axial force that the VA actually reflects the lag effect of the axial force transmission between the beams in each story. With the development of the displacement, the axial tension force is gradually transferred upward. The load–displacement curves of each model exhibit multiple relationships with the number of the stories in the flexural mechanism stage, whereas the VA leads to an uneven distribution of the internal forces in each story. Thus, the VA mainly affects the internal force redistribution of the multi-story frame and has ignored influence on the resistance. When a sudden load occurs, the failure story is destroyed easily, and the VA makes the stress of the beams in each story more uneven, which could cause the progressive collapse of the frame from the bottom to top stories. In addition, scholars have suggested adding steel strands [36] or steel cables [37] to the beams of single-story beam–column assemblies to increase the axial forces. However, as the internal force development law of multi-story frames is different from that of single-story beam–column assemblies, if these reinforcement measures are applied to multi-story frame, the collapse performance may not be improved as desired in the upper stories.

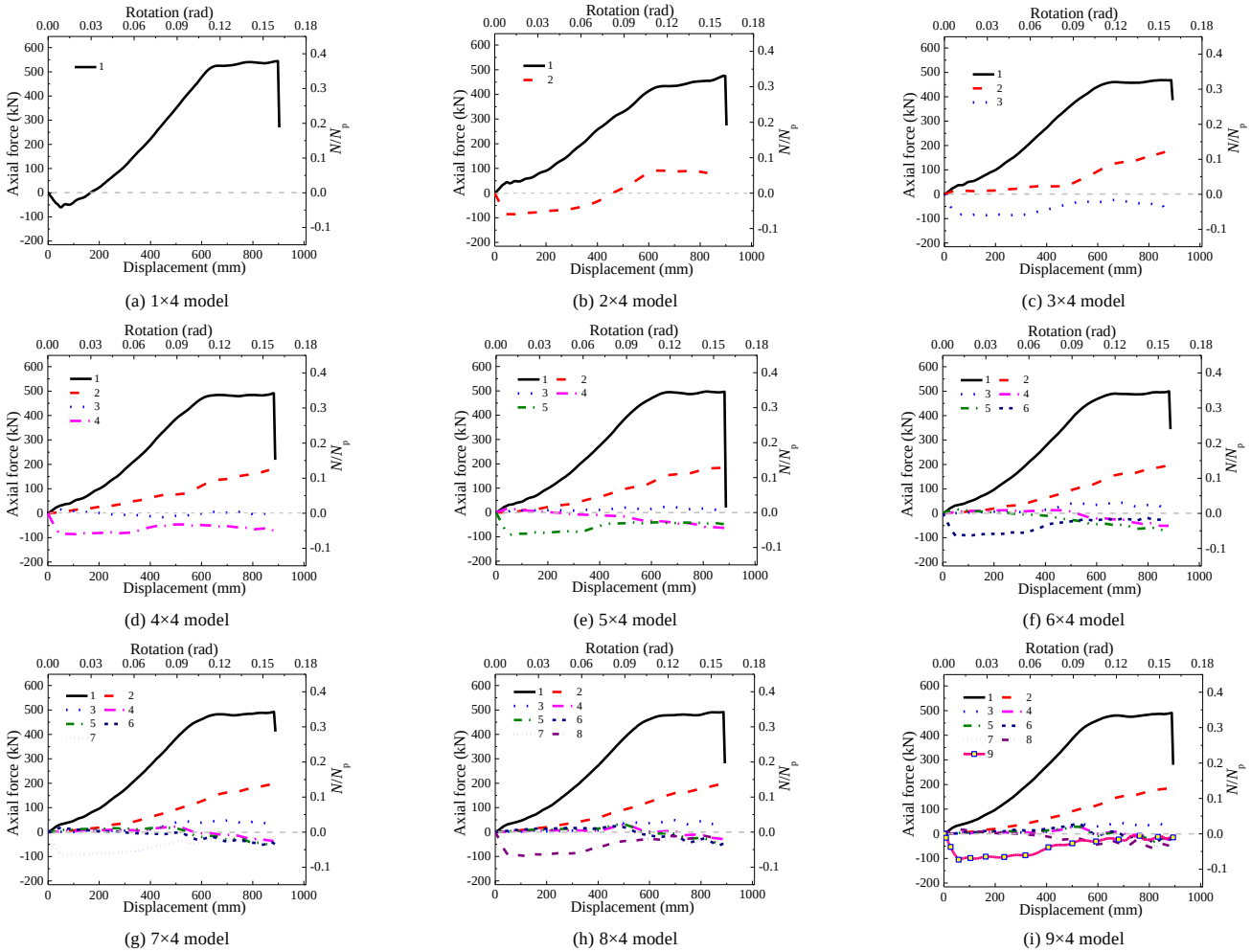

(a) 1×4 model (b) 2×4 model (c) 3×4 model

(d) 4×4 model (e) 5×4 model (f) 6×4 model

(g) 7×4 model (h) 8×4 model (i) 9×4 model

Fig. 11 Axial force of two-bay beams of each story

The bending moment development at the beam ends of the frame structures with different numbers of stories in the middle column removal scenario is illustrated in Fig. 12. The flexural capacities of the beams in each story decrease as the number of stories increases in the initial stage. Taking the 9 × 4 model as an example, when the failed column reaches the yielding displacement [38] (30 mm) of the model, the bending moments of the first and ninth stories are 170 and 142 kN·m, respectively, and the bending moment of the top-story beams is only 84% of that of the first-story beams, because of the lag effect of the rotation at the ends of each story beam. With the development of displacement, all models can reach the plastic bending moment (M_p). Except for the bending moment in the failure story, the bending moments of the other stories decrease slowly until the weakened flange of the first story breaks. The higher the floor in the multi-story frame, the greater the bending moment reduction. Fig. 12 shows that the failure story beams contribute the largest catenary mechanism resistance (CMR); similarly, their contribution to the total flexural mechanism of the structure is also greater than that of the beams in the other stories. Therefore, the failure story are the most important components of the multi-story frame in resisting external loads.

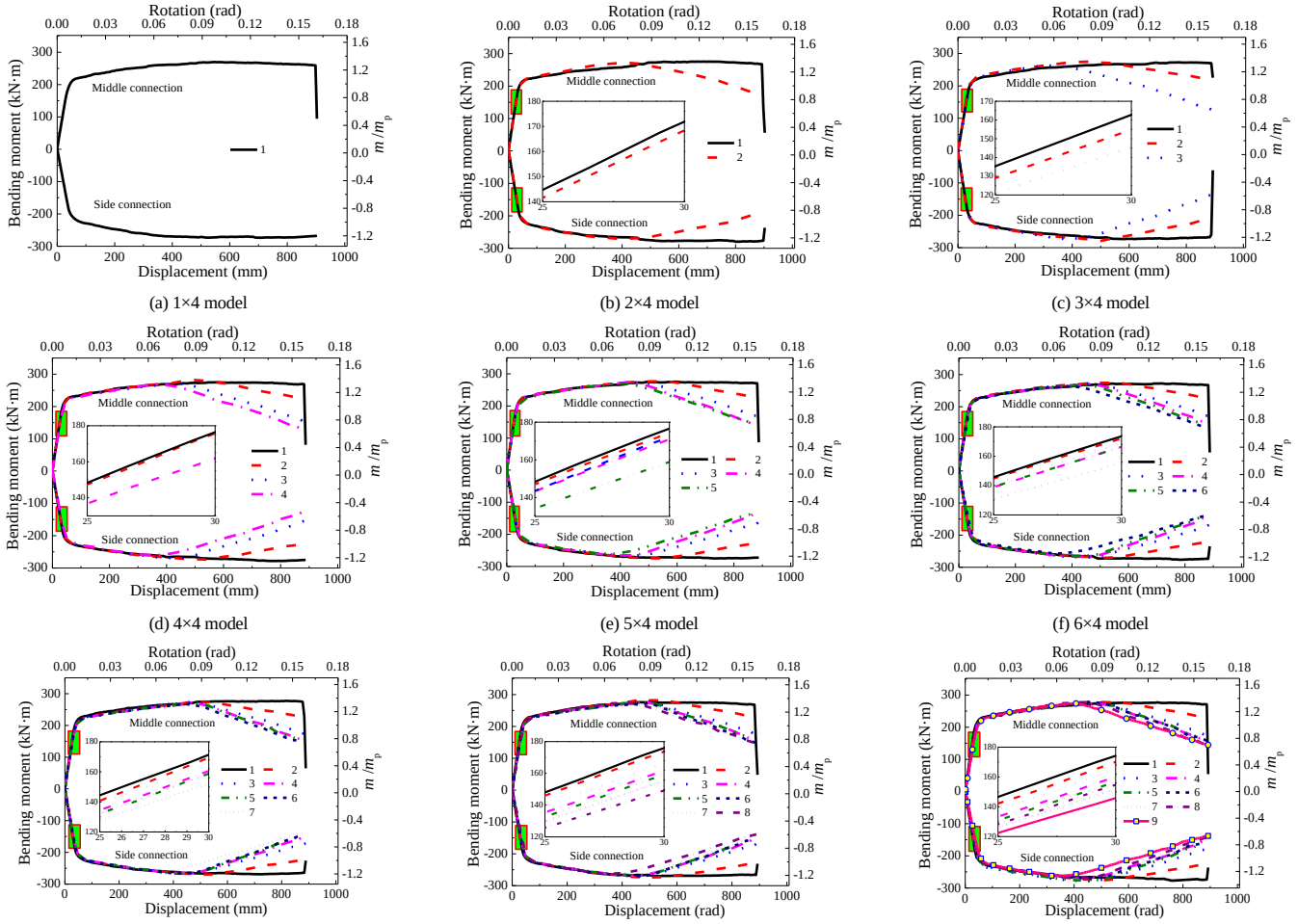

Fig. 12 Bending moment of beam ends at each story

3.3. Horizontal deformation characteristics of multi-story frames

Fig. 13 depicts the horizontal deformation characteristics of multi-story frames throughout the loading process. The horizontal displacement of the side connection of the outermost side column in the first and top stories are the smallest and largest, respectively. The horizontal displacement of the side connections in each story decreases with increasing number of stories, whereas the variations between the horizontal displacements of the stories above the third story are fairly small. This finding indicates that the horizontal restraint just only exerts the axial force effectively in the first through third stories, and the other stories cannot form effective axial tension forces. With the development of displacement, the outermost side column gradually exhibits s-shaped deformation characteristics.

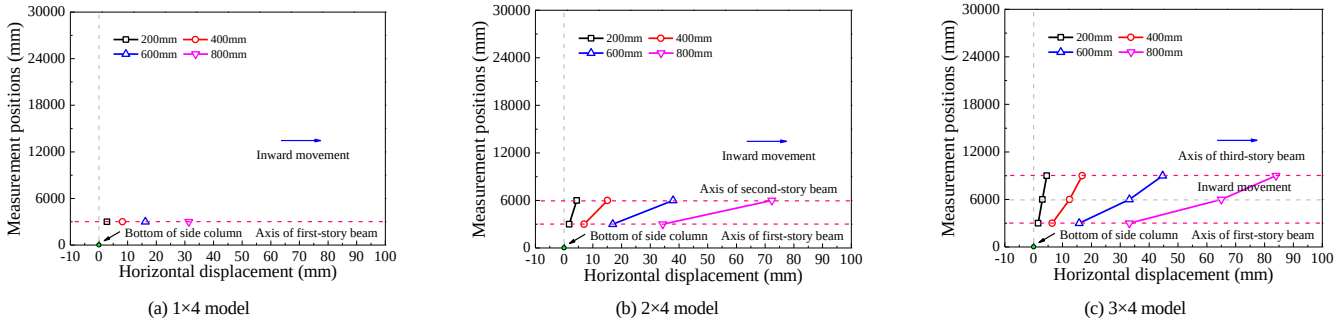

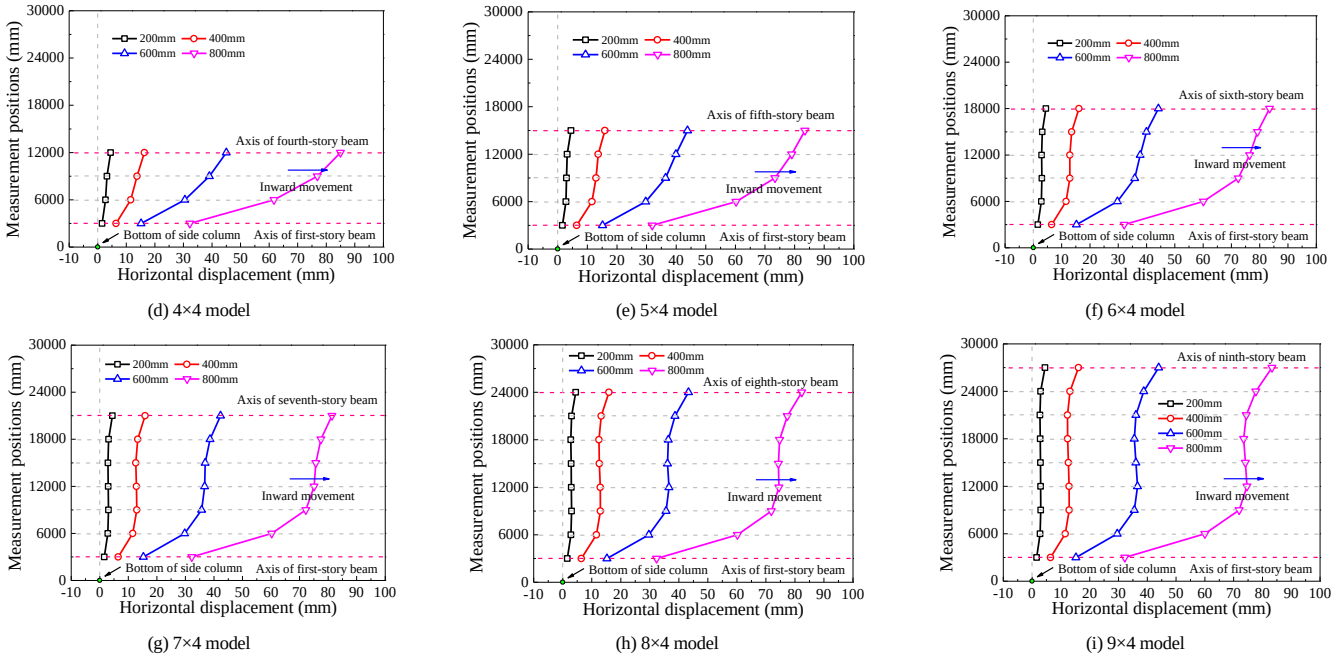

Fig. 13 Horizontal deformation characteristics of outermost side column

Eq. (5) and Fig. 14 show the boundary restraint constraint provided by the indirect area for the beam ends in each story in the direct area of the 9×4 model, where the stiffness mainly depends on the lateral stiffness of the restrained story (peripheral beams) and the peripheral columns and can be calculated by using Eq. (6). It is found that K_i decreases quickly with increasing number of stories and that the rapid decrease of the restraint effect mainly concentrated in the first three stories. The axial restraint stiffness for the beam ends at the fourth story is only 16% of that of the first story, which is consistent with the horizontal deformation characteristics shown in Fig. 13. The horizontal stiffnesses provided for the other stories are relatively small, which did not help effectively exert the catenary action of the two-bay beams in the upper stories. Thus, not all beams in different stories of a multi-story planar frame can exert the catenary action as well as two-bay beams in a one-story frame in the large deformation stage.

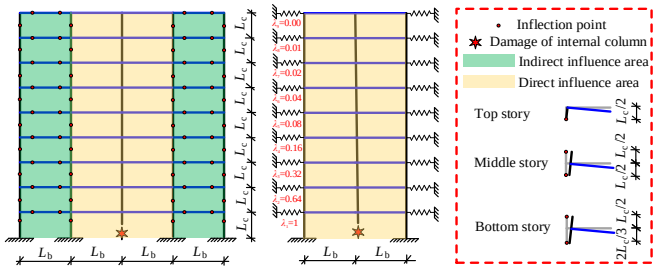

Fig. 14 Boundary restraint constraint of beam ends at each story in the direct area of model 9×4

$$K_i = 1/\sum_{i=1}^{n}(1/k_i) \tag{5}$$

$$k_i = 1/(1/k_{ci} + 1/k_b) \tag{6}$$

$$\lambda_i = K_i / K_1 \tag{7}$$

Here, K_i is the horizontal stiffness provided by the indirect area, k_{ci} is the horizontal stiffness [17] provided by the peripheral column, k_b is the horizontal stiffness [17] of the peripheral beam, and λ_i is the ratio of the axial stiffness in each story to that in the first story.

3.4. Analysis of different mechanism resistance development

Fig. 15 shows a force analysis diagram of the simplified model of each story of the multi-story frame structure. The total resistance of the frame is composed of the flexural mechanism resistance (FMR) and CMR. The FMR and CMR are composed of the vertical components of the shear and axial forces of the two-bay beams.

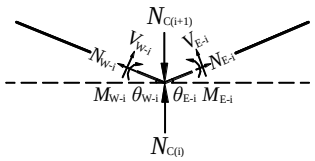

Fig. 15 Force analysis diagram of each story

The VA is actually the additional bending moment formed among the stories, although its contribution to the total resistance is too small and complex to separate, so it can be classified as the FMR. The FMR and CMR can be obtained from Eqs. (8) and (9). The contribution coefficients α_F and β_C of the FMR and CMR are given by Eqs. (10) and (11), where α_F is the sum of resistance contribution coefficient α_{Fi} of flexural mechanism of each story and β_C is the sum of resistance contribution coefficient β_{Ci} of catenary mechanism of each story. The collapse resistance provided by each story and its contribution coefficient η_i can be calculated using Eqs. (12) and (13), respectively. Based on the method of energy balance conversion [15], the resistance contribution coefficients α_F, β_C, α_{Fi}, and β_{Ci} are proposed, which are used to evaluate the quantitative contribution of the FMR and CMR in each story to the total resistance.

$$P_C = \sum P_{Ci} = \sum(2N_i \sin\theta_i) \tag{8}$$

$$P_F = P - P_C \tag{9}$$

$$\alpha_F = \sum \alpha_{Fi} = \sum(\int_0^v P_{Fdi}dv / \int_0^v P_{di}dv) \tag{10}$$

$$\beta_C = \sum \beta_{Ci} = \sum(\int_0^v P_{Cdi}dv / \int_0^v P_{di}dv) \tag{11}$$

$$P = N_{C(max)} = \sum P_i = \sum(N_{C(i+1)} - N_{C(i)}) = \sum(P_{Fi} + P_{Ci}) \tag{12}$$

$$\eta_i = \int_0^v P_{idi}dv / \int_0^v P_{di}dv \tag{13}$$

Here, N_i is the axial force of each story beam, θ_i is the rotation of the beam end of each story, P_i is the resistance provided by each story, P_{Fi} and P_{Ci} are the FMR and CMR of each story, respectively, $N_{C(max)}$ is the total resistance, and $N_{C(i+1)}$ and $N_{C(i)}$ are the axial forces of the steel columns in the $(i+1)^{th}$ and i^{th} floors, respectively.

Figs. 16(a) and (b) depict the FMR and CMR development curves of each model. The FMR development trend is consistent with the load-displacement

curve, and the structural load is provided entirely by the flexural mechanism in the small deformation stage. The CMR increases gradually with increasing number of stories, but the overall difference is not significant. This similarity exists because the catenary mechanism of the frame structures in the different stories is mainly provided by the bottom story, and the CMRs provided by the other stories are small. The higher the floor, the smaller the contribution of the catenary action. The resistance development of each model is mainly divided into two different stages: the flexural mechanism stage and the flexural mechanism–catenary mechanism mixed stage. There is no obvious catenary stage (the CMR exceeds the FMR and becomes the dominant mechanism resistance). Fig. 16(c) shows the contribution ratio between the FMR and CMR in the different stages in each model. As the number of stories increases, the conversion between the flexural and catenary mechanisms of the frame structure is delayed, which indicates that the conclusion obtained from the single-story frame will overestimate the CMR of the actual multi-story frame structure, resulting in a larger bearing capacity in the latter. Figs. 16(e) and (f) show the contribution coefficients α_F and β_C of FMR and CMR of each story. The contribution coefficients of the CMRs decrease continuously with increasing number of stories. For the frame structures with more than three stories, the frame relies heavily on the flexural mechanism to resist external load, and the contribution of the CMR is less than 10%.

3.5. Resistance development provided by each story

Fig. 17 shows the resistance development provided by each story in the multi-story frames with different numbers of stories. In the initial stage, the resistance of each story is basically identical. As the displacement increases, the curves start to diverge. As the catenary mechanism is mainly concentrated on the first story, the first story contributes the greatest resistance among the stories, followed by the second story, and then the third story. There is little difference in the resistances of the upper stories above the third story owing their similar CMRs, and Table 3 shows the specific resistance contribution coefficients of each story.

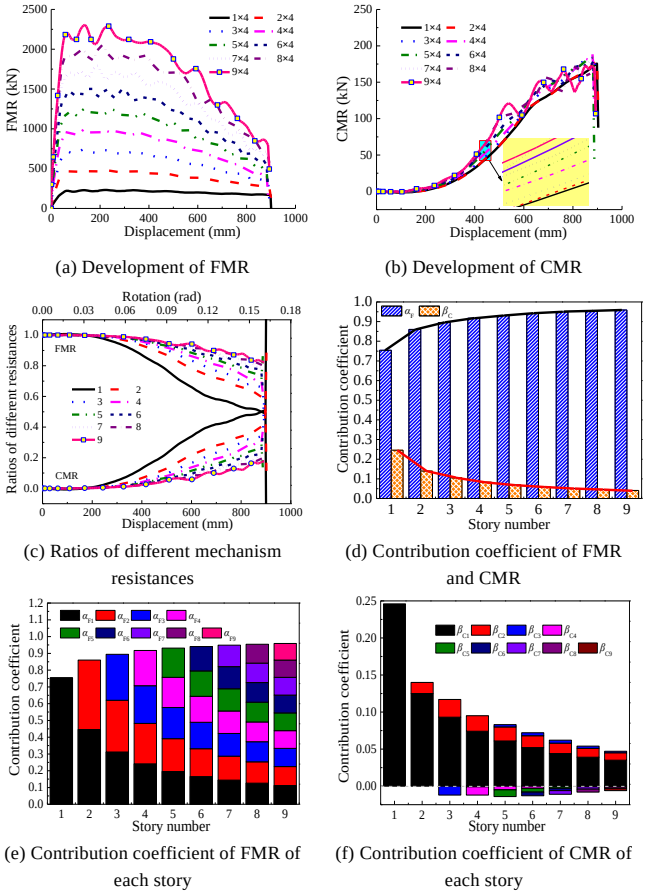

(a) Development of FMR (b) Development of CMR

(c) Ratios of different mechanism resistances (d) Contribution coefficient of FMR and CMR

(e) Contribution coefficient of FMR of each story (f) Contribution coefficient of CMR of each story

Fig. 16 Development of different mechanism resistance

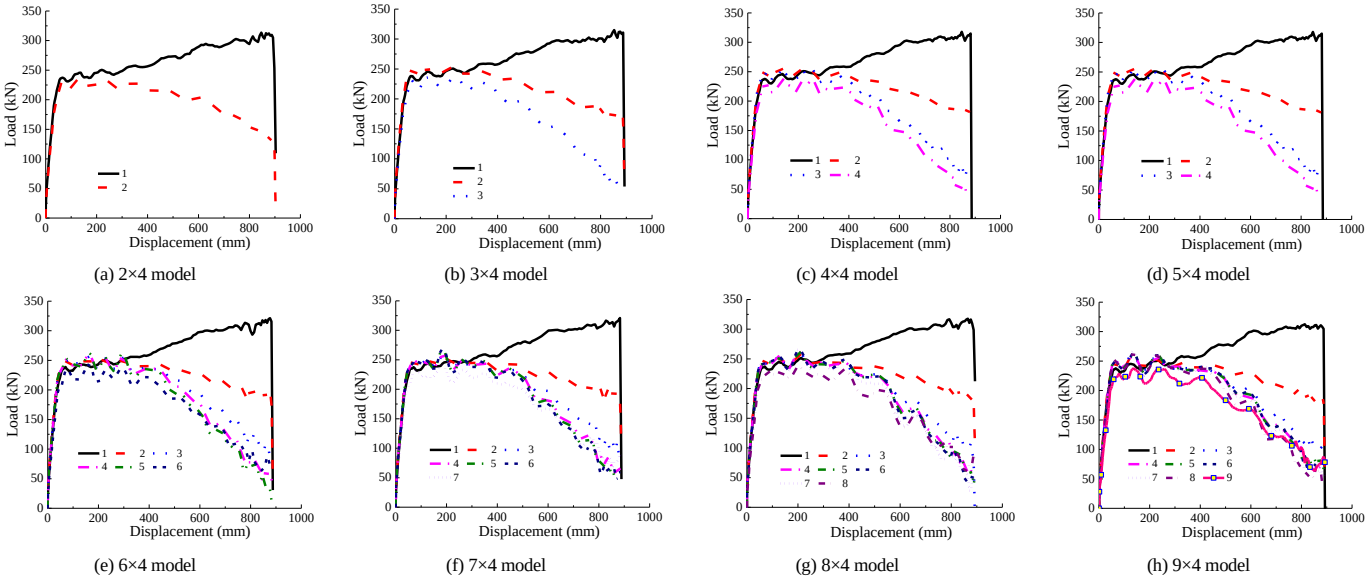

(a) 2×4 model (b) 3×4 model (c) 4×4 model (d) 5×4 model

(e) 6×4 model (f) 7×4 model (g) 8×4 model (h) 9×4 model

Fig. 17 Resistance development provided by each story

Table 3
Resistant contribution coefficients of each story

Models	η_1	η_2	η_3	η_4	η_5	η_6	η_7	η_8	η_9
1×4	1								
2×4	0.571	0.429							
3×4	0.406	0.332	0.262						
4×4	0.315	0.262	0.224	0.199					
5×4	0.256	0.215	0.189	0.175	0.165				
6×4	0.217	0.182	0.162	0.152	0.146	0.141			
7×4	0.188	0.157	0.139	0.133	0.131	0.129	0.123		
8×4	0.165	0.139	0.123	0.118	0.118	0.116	0.113	0.108	
9×4	0.147	0.123	0.110	0.106	0.106	0.106	0.105	0.101	0.096

4. Collapse resistances of frames with different numbers of spans

To comprehensively analyze the effect of the number of spans on the collapse resistances of the frame structure further, the one-, three- and nine-story frames with 2, 4, 6, 8, and 10 spans were employed to study the influence of the peripheral frames in the indirect area on the structural behavior of the failure frame in the direct area upon internal column removal.

4.1. Load–displacement response

Fig. 18 shows the load-displacement response of the one-, three- and nine-story frame structures with different numbers of spans upon middle column removal. With increasing number of spans, the initial stiffness and plastic load of the structures are basically the same. With increasing displacement of the failed column, the curves of the models start to diverge, and the models with 10 spans (the 1×10, 3×10, and 9×10 models) achieve greater load-resisting capacities in the larger deformation stage than those with fewer spans, but increasing number of spans was not conducive to the displacement development. Increasing the number of spans has large effects on the frames with few stories, such as the one- and three-story frames (see Figs. 18(a) and (c)), whereas the structural collapse resistance of the nine-story frame exhibits only very limited improvement, as shown in Fig. 18(c).

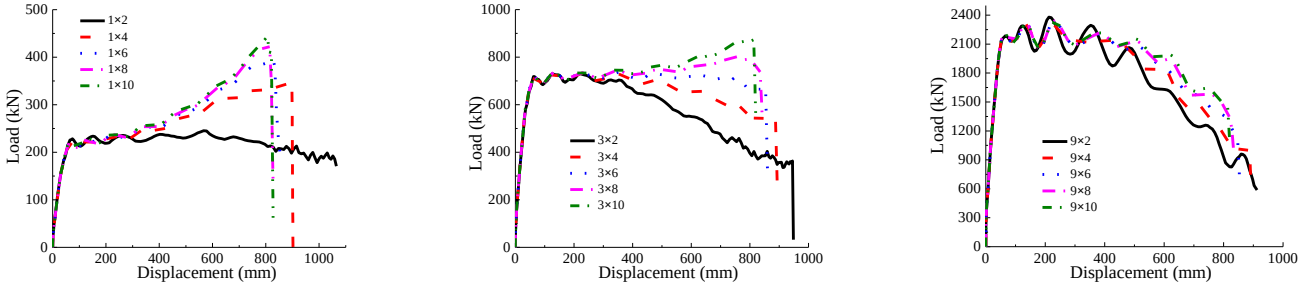

(a) One-story frames (b) Three-story frames (c) Nine-story frames

Fig. 18 Load response of frame structure with different span numbers

4.2. Demand analysis of peripheral frames

Fig. 19 illustrates the axial force development of the 1×10, 3×10, and 9×10 models. The axial force in the first story of the 1×10 model reaches $0.86N_p$, whereas the axial forces of 3×10 and 9×10 models in the first story can only reach $0.60N_p$ and $0.59N_p$, respectively. The axial forces in each beam along the inside-out and bottom-up directions (pink arrows) tend to decrease gradually, as presented in Fig. 19(c). It can be clearly seen that the axial forces of the peripheral beams in the first story of the 1×10 model are twice those in the 3×10 model, whereas the axial forces in the bottom three stories in the 3×10 and 9×10 models are basically the same, which indicates that the peripheral beams above the third story exert limited restraint forces on the frame in the direct area. Thus, the collapse resistances of multi-story, multi-span frames can be analyzed and evaluated using the results obtained from beam-column assemblies with different boundary conditions.

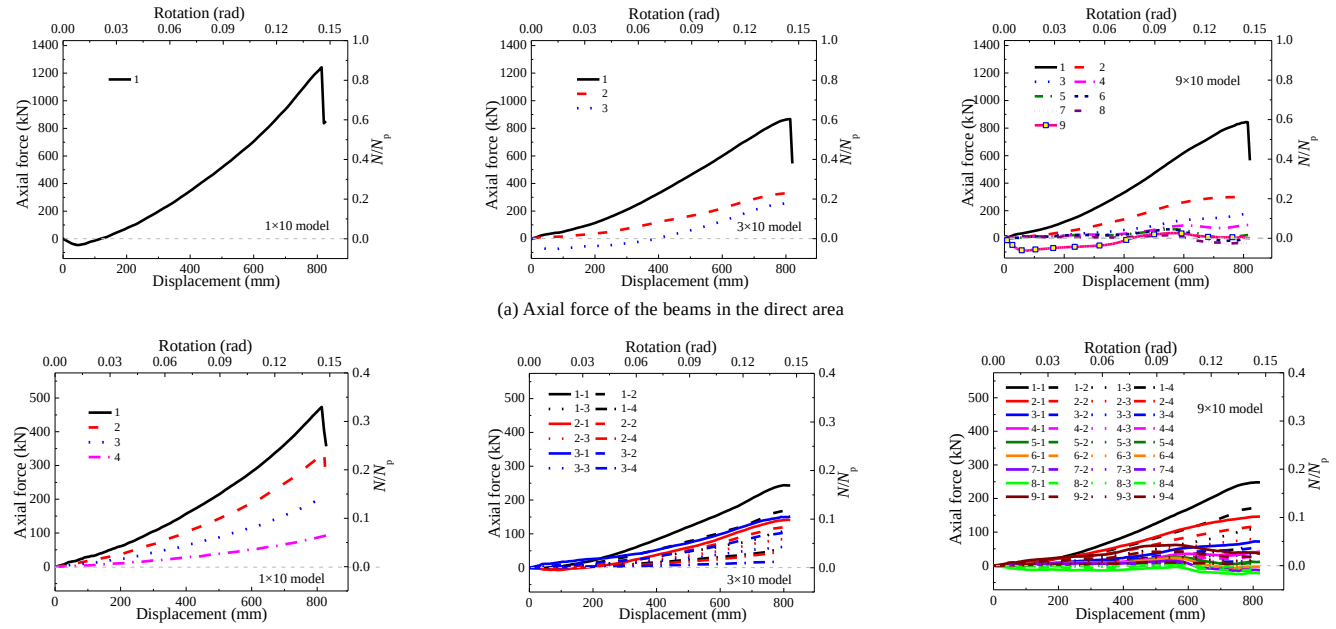

(a) Axial force of the beams in the direct area

(b) Axial force of the peripheral beams in the indirect area

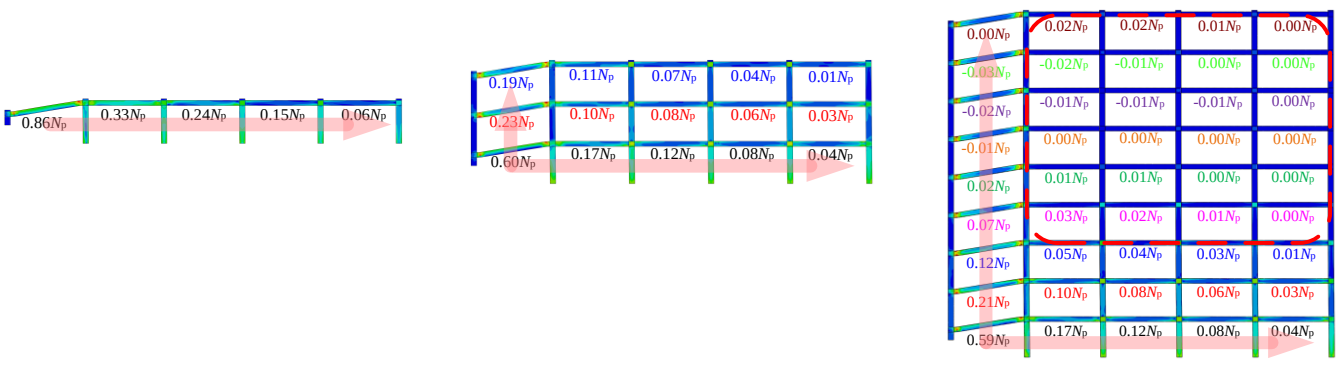

(c) Axial force distribution in beams of frame

Fig. 19 The axial forces development of each beam

4.3. Evolution law of the internal forces among the stories

The nine-story frames are more typical and meaningful than the one- and three-story frames in the analysis of anti-progressive collapse behavior; thus, the nine-story frames were used as examples to elaborate the effects of the number of spans on the collapse behavior. Fig. 20 illustrates the axial force development of each beam in the nine-story frames with different span numbers. As the number of spans increases, the axial forces in the first- through sixth-story beams increase continuously and increasing the number of spans will accelerate the upward transmission of the axial tension force in each story. The axial compression force in the top story decreases with increasing number of spans, as depicted in Fig. 20(g), which indicates that increasing the number of spans is not conductive to retaining compression of the top story and causes the VA to disappear. All the steel beams in the first stories of the different models are always in tension, indicating that there is no obvious compression arch action in the model, which may be related to the RBS connection. Similarly, the axial forces in the first stories of the two frames with RBS connections in the collapse tests verified above do not exhibit negative values. The axial force of the second story beam of each model is negligible during the initial stage of loading. With increasing displacement, the axial force increases slowly. For the models with two, four, and six spans, the axial forces of the third story are negative, whereas the third-story axial forces are positive for the other three models. Therefore, the axial force is gradually transferred upward as the displacement changes. Further, as the number of spans increases, the upward transmission of the axial force in each story is accelerated. Figs. 13(i) and 21 illustrate the development of bending moments at each story beam ends of the frames with different numbers of spans. The attenuation trend and amplitude of the bending moment remain constant as the number of spans changes, which shows that the flexural capacities of each story are not affected by the peripheral restraints.

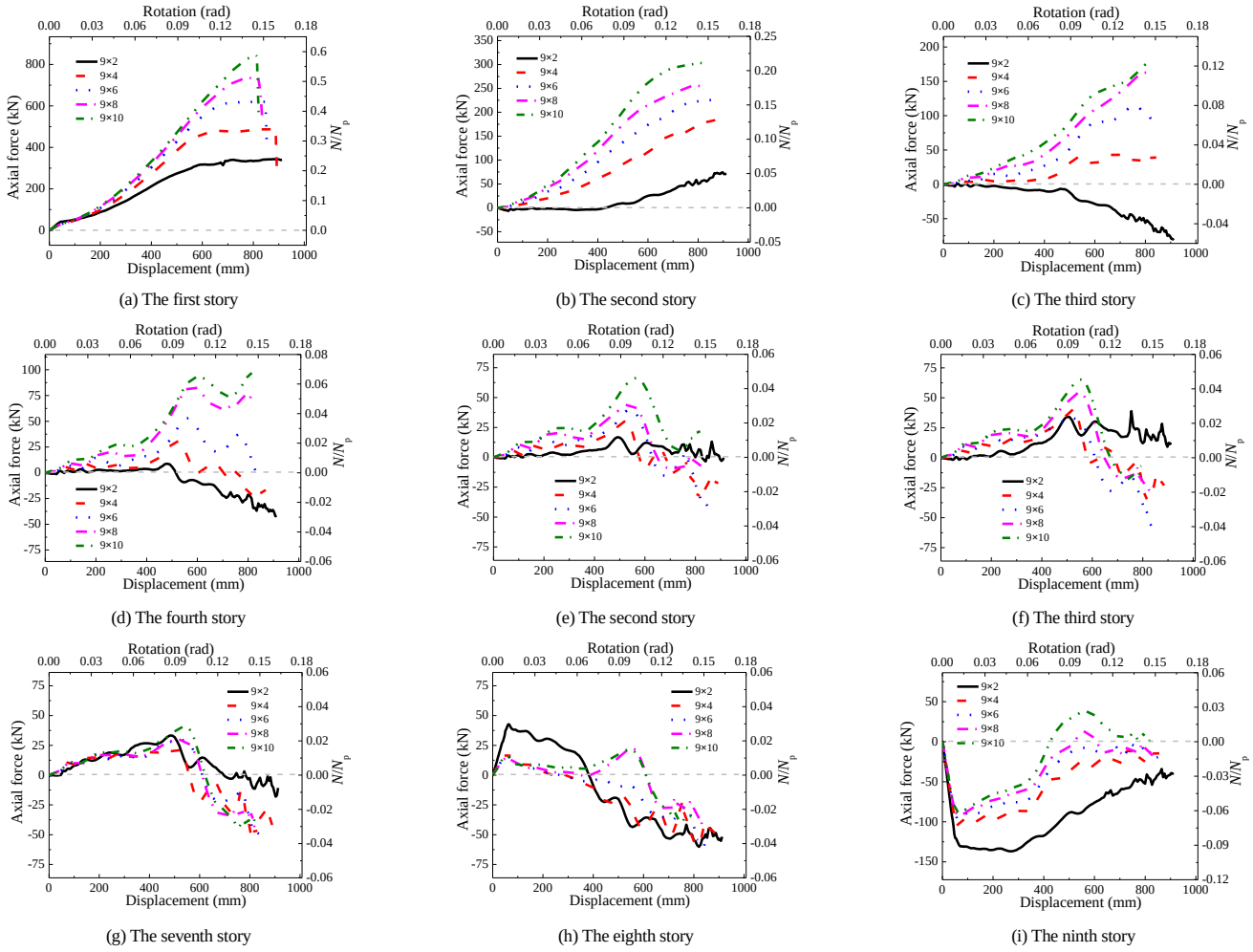

Fig. 20 Axial forces of each story beams

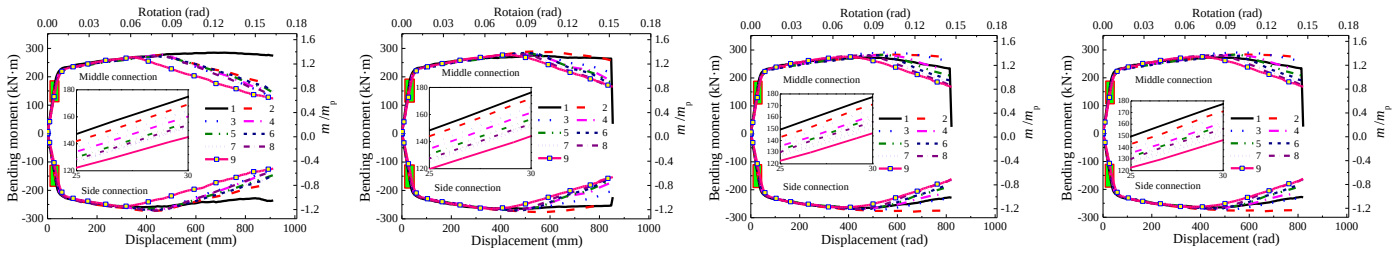

Fig. 21 Bending moment of beam ends at each story

4.4. Horizontal deformation characteristics of multi-story frames

Fig. 22 shows the horizontal deformation shape of the outermost column of each model throughout the loading process. The horizontal displacement at the first-floor side joints is the smallest, followed by that of the second-floor joints, and the differences in the horizontal displacements of the side connections above the third floor are small. With increasing number of spans around the failed column, the horizontal displacements of the side joints in each story decrease. It can be seen that the fewer the spans, the more significant the s-shape of the deformation characteristics of the structure.

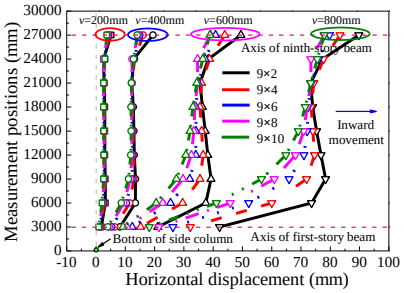

Fig. 22 Horizontal deformation characteristics of outermost column

4.5. Resistance development curve of different mechanisms

Figs. 23(a) and (b) show the development curves of the FMR and CMR of each model. The FMRs of the models are similar, whereas the CMRs increase with increasing number of spans. Fig. 23(c) depicts the contribution ratio between the FMR and CMR in different stages for each model, demonstrating that increasing the number of spans will accelerate the transformation from flexural mechanism to catenary mechanism. As shown in Fig. 23(d), with the increasing of the number of spans, the FMR contribution decreases and the CMR contribution increases. Figs. 23(e) and (f) present the FMR and CMR contributions of each story α_F and β_C. The CMR contribution coefficients are less than 10%, indicating that the total resistance was mainly provided by the flexural mechanism throughout the loading process for the high-rise buildings.

4.6 Resistance development provided by each story

Fig. 24 illustrates the collapse resistance development of each story beam in the models with different numbers of spans. The resistance provided by each story is basically identical in the small deformation stage, then starts to diverge. Overall, the failure and top stories contribute the maximum and minimum resistances, respectively. The differences in the total resistances of the models are mainly reflected in the first, second, and third stories, whereas there was no remarkable difference in the resistance in the other stories. The resistance contribution coefficients of each story of each model, as lists in Table 4. Increasing the number of spans can enhance the ability of the stories above the failure story to resist the external load, and the corresponding contribution coefficients increase continuously until close to the resistance contribution coefficient of each story. Thus, if the boundary restraints are sufficiently large so that each story is independent of the others and there is no interaction among the stories, the resistance provided by each story would be equal, and each story beam would account for 1/*n* to the total resistance.

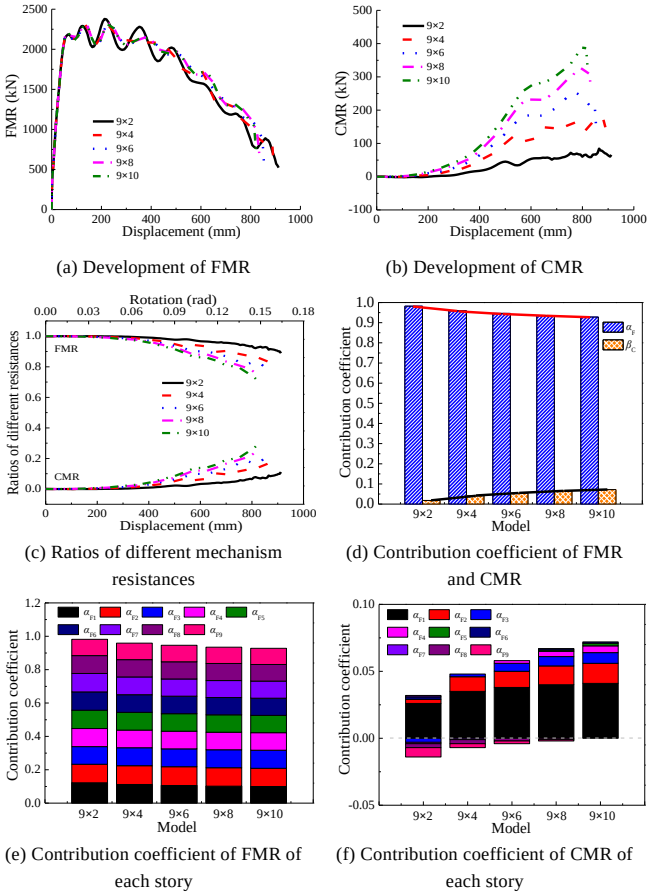

(a) Development of FMR
(b) Development of CMR
(c) Ratios of different mechanism resistances
(d) Contribution coefficient of FMR and CMR
(e) Contribution coefficient of FMR of each story
(f) Contribution coefficient of CMR of each story

Fig. 23 Development of different mechanism resistances

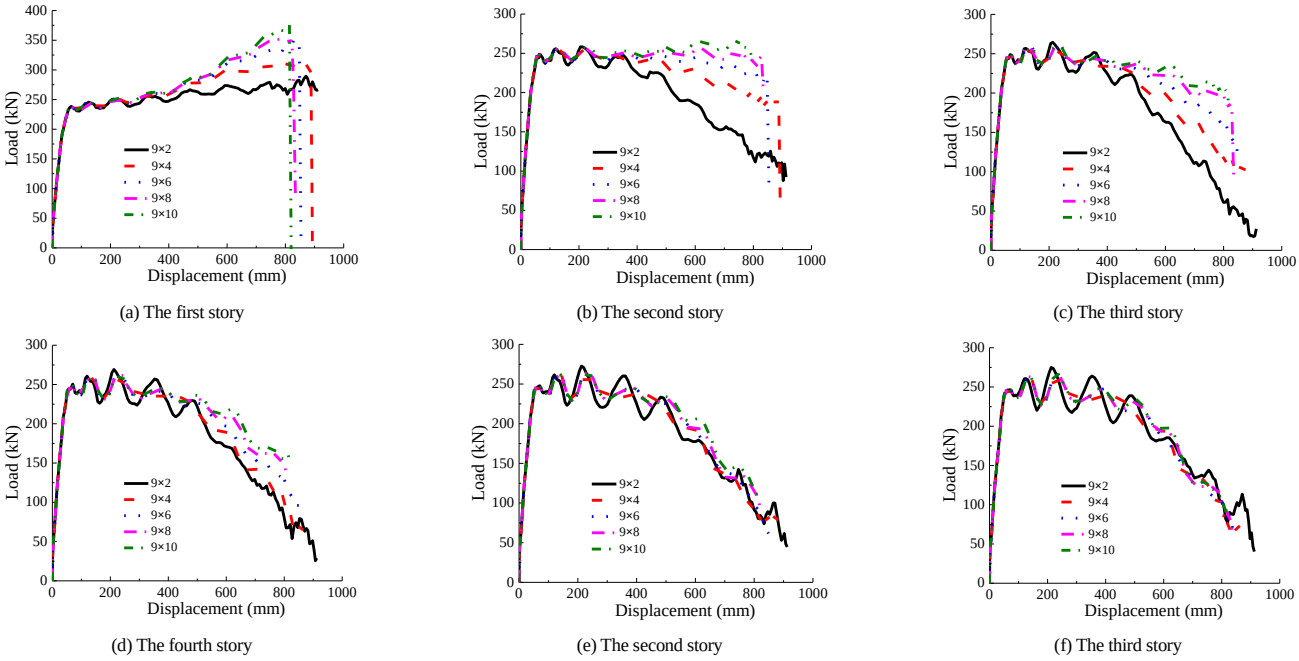

(a) The first story
(b) The second story
(c) The third story
(d) The fourth story
(e) The second story
(f) The third story

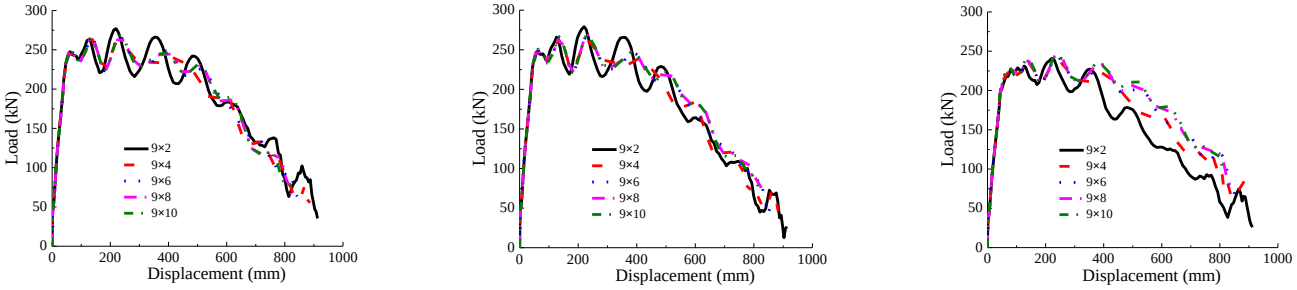

(g) The seventh story (h) The eighth story (i) The ninth story

Fig. 24 Development of resistance provided by each story

Table 4
Resistant contribution coefficients of each story

Models	η_1	η_2	η_3	η_4	η_5	η_6	η_7	η_8	η_9
9×2	0.148	0.114	0.103	0.107	0.110	0.112	0.111	0.104	0.091
9×4	0.147	0.123	0.110	0.106	0.106	0.106	0.105	0.101	0.096
9×6	0.144	0.124	0.113	0.108	0.105	0.105	0.103	0.101	0.097
9×8	0.142	0.124	0.115	0.109	0.105	0.105	0.102	0.101	0.097
9×10	0.141	0.124	0.116	0.110	0.106	0.104	0.102	0.100	0.097

5. Conclusion

In this study, multi-story plane frame structures with RBS connections were taken as the research object. Using a refined finite element modeling method, nonlinear analysis models were established to investigate the collapse resistance performance of the multi-story and multi-span frame structures. The collapse resistances, internal force distributions, deformation characteristics, and load-resisting mechanisms were analyzed comprehensively, and the contributions of the respective mechanisms of each story in the steel frame were quantified separately. The conclusions drawn in this study were:

(1) The collapse resistances of the most common two-bay, single-story frames and actual multi-story frames do not follow simple multiple relationships with the number of stories. Increasing the number of stories is not conducive to the exertion of the catenary mechanism in the upper stories, and it is not appropriate to apply the analysis results for a single-story frame structure to the collapse resistant designs of multi-story structures. Thus, it is unreasonable to replace actual multi-story frame structures directly with single-story frames to analyze the progressive collapse resistance.

(2) The VA was present in the multi-story frames, which had both favorable and unfavorable effects on the collapse performances of the structures. The VA could slightly improve the bearing capacity of the frame in the flexural mechanism stage. However, it also led the uneven distribution of internal forces among the stories, and the strength of the upper stories, in which more external load was resisted by the beams above the failed column, was not fully utilized. This characteristic will increase the risk of progressive collapse and make frame structures undergo progressive collapse from the failure story to the top story.

(3) The existence of the VA actually reflects the overall mechanical behavior of the multi-story frame in the process of internal force redistribution, but the VA has negligible influence on the structural resistance in the small deformation stage.

(4) With increasing number of stories, the restraint action of the beams peripheral to the frame in the direct area decreases according to a quadratic curve. The rapid decrease in the restraint action is mainly concentrated in the first three stories, whereas the horizontal restraint stiffness at the beam ends of the fourth story is only 16% of that of the first story. In addition, the first three stories above the failed story exhibited the largest differences, whereas there were minimal differences between the other stories. Therefore, the total resistance of a multi-story frame is roughly equivalent to the sum of the resistances of single-story frame with different horizontal restraint stiffnesses.

(5) The boundary constraint plays an important role in the structural behavior of a multi-story frame, as reflected in the influences of the internal force redistribution among floors and catenary mechanism resistance. Increasing the number of spans significantly affects the catenary mechanism resistance of frames with few stories, whereas it has little effect for the frames with more stories. For high-rise buildings, the total resistance was mainly provided by the flexural mechanism, whereas the catenary mechanism contributed little and mainly occurred in the beams closer to the failure story.

It should be noted that the effects of the floor slab action and spatial action on the structural behavior were ignored in this study, which should be carried out in future research.

Acknowledgments

This research was supported by the National Natural Science Foundation of China [grant numbers 51678476, 51608433, 51908449], Scientific research plan projects of the Shaanxi Education Department [grant number 20JY033, 20JK0713]. All opinions, findings, conclusions, and recommendations expressed in this paper are those of the authors and do not necessarily reflect the views of the sponsors.

References

[1] UFC 4-023-03. Design of structures to resist progressive collapse, Department of Defense, Washington, D.C., USA, 2013.
[2] Tian L.M., Wei J.P., Hao J.P., “Method for evaluating the progressive collapse resistance of long-span single-layer spatial grid structures”, Advanced Steel Construction, 15(1): 109-115, 2019.
[3] Tian L.M., He J.X., Zhang C.B., et al., “Progressive collapse resistance of single-layer latticed domes subjected to non-uniform snow loads”, Journal of Constructional Steel Research, 176: 106433, 2021.
[4] Zhang Y.R., Wei Y., Bai J.W., et al., “A novel seawater and sea sand concrete filled FRP-carbon steel composite tube column: Concept and behavior”, Composite Structures, 246: 112421, 2020.
[5] Tan Z., Zhong W.H., Tian L.M., et al., “Research on the collapse-resistant performance of composite beam–column substructures using multi-scale models”, Structures, 27: 86–101, 2020.
[6] Dinu F., Marginean I., Dubina D., “Experimental testing and numerical modelling of steel moment-frame connections under column loss”, Engineering Structures, 151: 861–878, 2017.
[7] Yang B., Tan K.H., “Experimental tests of different types of bolted steel beam-column joints under a central-column-removal scenario”, Engineering Structures, 54: 112–130, 2013.
[8] Meng B., Li L.D., Zhong W.H., et al., “Enhancing collapse-resistance of steel frame joints based on folded axillary plates”, Advance Steel Construction, 17(1): 84–94, 2021.
[9] Gao S., Xu M., Guo L.H., et al., “Behavior of CFST-column to steel-beam joints in the scenario of column loss”, Advance Steel Construction, 15(1): 47–54: 2019.
[10] Kang S.B., Tan K.H., Liu H.Y., et al., “Effect of boundary conditions on the behaviour of composite frames against progressive collapse”, Journal of Constructional Steel Research, 138: 150–167, 2017.
[11] Weng J., Lee C.K., Tan K.H., et al., “Damage assessment for reinforced concrete frames subject to progressive collapse”, Engineering Structures, 149: 147–160, 2017.
[12] Wang W., Wang J., Sun X., et al., “Slab effect of composite subassemblies under a column removal scenario”, Journal of Constructional Steel Research, 129: 141–155, 2017.
[13] Alashker Y., El-Tawil S., “A design-oriented model for the collapse resistance of composite floors subjected to column loss”, Journal of Constructional Steel Research, 67: 84–92, 2010.
[14] Yu J., Tan K.H., “Structural behavior of RC beam-column sub-assemblages under a middle column removal scenario”, Journal of Structural Engineering, 139(2): 233–250, 2013.
[15] Tan Z., Zhong W.H., Tian L.M., et al., “Quantitative assessment of resistant contributions of two-bay beams with unequal spans”, Engineering Structures, 242: 112445, 2021.
[16] Zhong W.H., Tan Z., Tian L.M., et al., “Collapse resistance of composite beam-column assemblies with unequal spans under an internal column-removal scenario”, Engineering Structures, 206: 110143, 2020.
[17] Zhong W.H., Tan Z., Song X.Y., et al., “Anti-collapse analysis of unequal span steel beam-column substructure considering the composite effect of floor slabs”, Advance Steel Construction, 15(4): 377–385, 2019.
[18] Stinger S.M., Orton S.L., “Experimental evaluation of disproportionate collapse resistance in reinforced concrete frames”, ACI Structural Journal, 110(3): 521–529, 2013.
[19] Elsanadedy H.M., Almusallam T.H., Al-Salloum Y.A., et al., “Investigation of precast RC

beam-column assemblies under column loss scenario", Construction Building Material, 142: 552–571, 2017.
[20] Tan Z., Zhong W.H., Tian L.M., et al., "Numerical study on collapse-resistant performance of multi-story composite frames under a column removal scenario", Journal of Building Engineering, 44: 102957, 2021.
[21] Li G.Q., Zhang J.Z., Jiang J., "Multi-story composite framed-structures due to edge-column loss", Advance Steel Construction, 16(1): 20–29, 2020.
[22] Yi W.J., He Q.F., Xiao Y., et al., "Experimental study on progressive collapse-resistant behavior of reinforced concrete frame structures", ACI Structural Journal, 105(4): 433–439, 2008.
[23] Baghi H., Oliveira A., Valencac J., et al., "Behavior of reinforced concrete frame with masonry infill wall subjected to vertical load", Engineering Structures, 171: 476–487, 2018.
[24] Wang F.L., Yang J., Pan Z.F., "Progressive collapse behaviour of steel framed substructures with various beam-to-column connections", Engineering Failure Analysis, 109: 104399, 2020.
[25] Qian K., Lan X., Li Z., et al., "Progressive collapse resistance of two-storey seismic configured steel sub-frames using welded connections", Journal of Constructional Steel Research, 170: 106117, 2020.
[26] Tsitos A., Mosqueda G., Filiatrault A., et al., "Experimental investigation of progressive collapse of steel frames under multi-hazard extreme loading", In The 14th World Conference on Earthquake Engineering, Beijing, China, 2008.
[27] Chen J.L., Huang X., Ma R.L., et al., "Experimental study on the progressive collapse resistance of a two-story steel moment frame", Journal of Performance of Constructed Facilities, 26(5): 567–575, 2012.
[28] Sasani M., Sagiroglu S., "Gravity load redistribution and progressive collapse resistance of a 20-story reinforced concrete structure following loss of an interior column", ACI Structural Journal, 107(6): 636–644, 2010.
[29] Tian L.M., Wei J.P., Huang Q.X., et al., "Collapse-resistant performance of long-span single-layer spatial grid structures subjected to equivalent sudden joint loads", Journal of Structural Engineering. 147(1): 04020309, 2021.
[30] Tian L.M., Kou Y.F., Lin H.L., et al., "Interfacial bond–slip behavior between H-shaped steel and engineered cementitious composites (ECCs)", Engineering Structures, 231: 111731, 2021.
[31] GB 50017-2017. Standard for design of steel structures, China Architecture & Building Press, Beijing, China, 2017.
[32] ANSI/AISC 358-10. Prequalified Connections for Special and Intermediate Steel Moment Frames for Seismic Applications, AISC; 2014.
[33] ABAQUS. Abaqus Analysis User's Guide (6.14), ABAQUS Inc.; 2014.
[34] Yu H.L., Jeong D.Y., "Application of a stress triaxiality dependent fracture criterion in the finite element analysis of unnotched Charpy specimens", Theoretical and Applied Fracture Mechanics, 54(1): 54–62, 2010.
[35] Izzuddin B.A., Vlassis A.G., Elghazouli A.Y., et al., "Progressive collapse of multi-storey buildings due to sudden column loss – Part I: Simplified assessment framework", Engineering Structures, 30(5): 1308–1318, 2008.
[36] Lu X.Z., Zhang L., Lin K.Q., et al., "Improvement to composite frame systems for seismic and progressive collapse resistance", Engineering Structures, 186: 227–242, 2019.
[37] Qiu L., Lin F., Wu K.C., "Improving progressive collapse resistance of RC beam-column subassemblages using external steel cables", Journal of Performance of Constructed Facilities, 34(1): 04019079, 2020.
[38] Feng P., Qiang H.L., Ye L.P., "Discussion and definition on yield points of materials, members and structures", Engineering Mechanics, 34(3): 36–46, 2017.